

## Long range dicorrelated stopping of relativistic electrons in ultradense plasmas

C. Deutsch and P. Fromy

Laboratoire de Physique des Gaz et Plasmas (CNRS-UMR No. 8578) and Centre de Ressources Informatiques, Bâtiment 210, Université Paris XI, 91405 Orsay, France

(Received 29 October 1999)

Fundamental features of dynamically dicorrelated relativistic electrons in the MeV energy range that interact with very dense and hot hydrogenic plasmas of fusion interest are thoroughly investigated. The target is modeled with a Drudelike dielectric function. Longitudinal and undamped pair correlations along overall drift velocity are contrasted to transverse ones decaying exponentially over several tens of target screening length  $\lambda_D$ . Other novel behaviors include a much higher response to target temperature variations than to density ones for the ratio of dicorrelated to uncorrelated stopping.

PACS number(s): 52.40.Mj, 52.50.Jm, 52.50.Lp

### I. INTRODUCTION

In the field of inertially confined thermonuclear fusion (ICF) one presently witnesses a strong interest in basic physics issues relevant to the interaction of laser produced and intense relativistic electron beams (REBs), in the MeV energy range, with precompressed hydrogenic deuterium + tritium fuel [1,2].

Corresponding target parameters highlight a rather extreme range:  $1 \leq T_e \leq 20$  keV and  $10^{25} \leq n_e \leq 10^{28}$  e cm<sup>-3</sup>. It has already been noticed [2] that an isolated electron projectile essentially loses energy through inelastic collisions with target electrons and the excitation of Langmuir collective modes. On the other hand, quasielastic deflections on target ions monitor an erratic projectile range, much longer than the effective REBs penetration depth [2].

Here, we intend to stress the quantitative significance of local target polarization when two projectiles fly in close vicinity of each other in the precompressed hydrogenic fuel.

Extensive and previous studies dedicated to nonrelativistic ion projectiles in much more dilute fully ionized and hydrogenic plasmas [3,4] have already demonstrated that a collective excitation due to a tagged projectile can modify the stopping performances of nearby projectiles thus experiencing a surfing (wake) effect rather well documented in cold targets [5,6]. If one considers a given dynamically dicorrelated projectiles pair, one observes alternatively positive and negative interferences in the energy loss processes. They are comparable, in absolute value, to the isolated projectile losses, on most of its velocity range. In the case of nonrelativistic ion projectiles, the correlation effects remain noticeable as long as the pair interdistance is smaller than the target electron screening length  $\lambda_D$ . When one turns his attention to relativistic electron projectiles, one is surprised to witness a similar dicorrelated stopping effect, but for pair interdistances larger than  $\lambda_D$ . This unexpected behavior is indeed confirmed by working out the relevant correlated stopping within an appropriate impact formalism proposed some time ago by Rule and Cha [7] along the lines of relativistic stopping for isolated particles with large impact parameter collisions, outlined previously by Fermi [8] and Jackson [9].

In the present work we intend to stress the basic properties of dicorrelated stopping for relativistic electron pairs in

hydrogenic targets of ICF interest. Then, we think it possible to elaborate a coherent formalism for  $N$ -correlated stopping with  $N \geq 2$  for a given REB of practical significance.

Relativistic two-electron stopping as formulated in Ref. [7] is briefly recalled in Sec. II. The resulting impact expression for correlated stopping is detailed in Sec. III. The hydrogenic target plasma is given a dispersionless Drudelike dielectric function in Sec. IV. Numerical results for the ratios of dicorrelated to uncorrelated relativistic stopping are explained in Sec. V and summarized in Sec. VI.

### II. BASIC FORMALISM

Two electron projectiles in close proximity ( $R_{12} \leq V\omega_p$ ) to each other may combine their separate stopping through target polarization. Following Jackson's [9] discussion of the Bohr method, we write the total work done on an atom in the medium by a passing cluster of particles as [7,8]

$$\Delta E = \int_{-\infty}^{\infty} dt \int \vec{E} \cdot \vec{j} d^3x. \quad (1)$$

In the usual way, this can be written in terms of Fourier transforms in frequency as

$$\Delta E = \frac{1}{2\pi N} \text{Re} \int_0^{\infty} (-i\omega) [i\varepsilon(\omega)|\vec{E}|^2 + \mu(\omega)|\vec{H}|^2] d\omega, \quad (2)$$

having introduced the linear relations

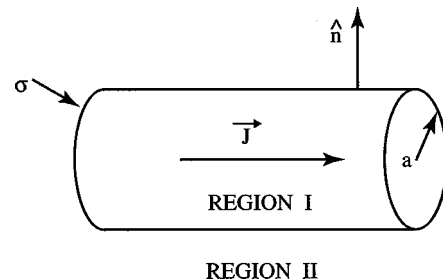


FIG. 1. The separation of the target plasma medium into a close-collision part and a distant-collision part. The vectors  $\vec{n}$  and  $-\vec{n}$  are unit normals to the surface  $\sigma$  surrounding the current  $\vec{j}$ . Here the separation distance  $a$  is taken equal to the plasma target screening length  $\lambda_D$ .

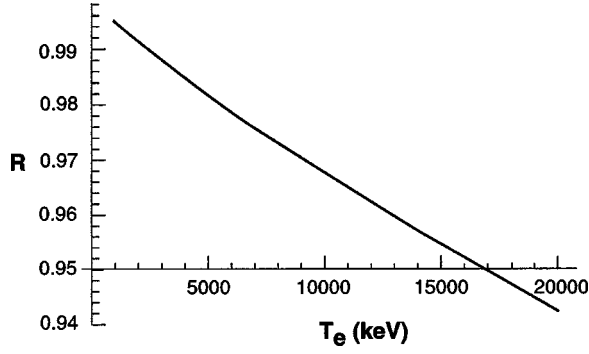


FIG. 2. Dicorrelated stopping ratio  $R$  [Eq. (20)] for a projectile electron pair with interdistances  $r_{\parallel}=r_{\perp}=1\lambda_D$  taken (respectively) parallel and transverse to overall drift velocity  $V=0.96c$ , flowing in a hydrogenic plasma with  $n_e=10^{26}e\text{ cm}^{-3}$ .  $R$  is given in terms of target electron temperature  $T_e$  (keV).

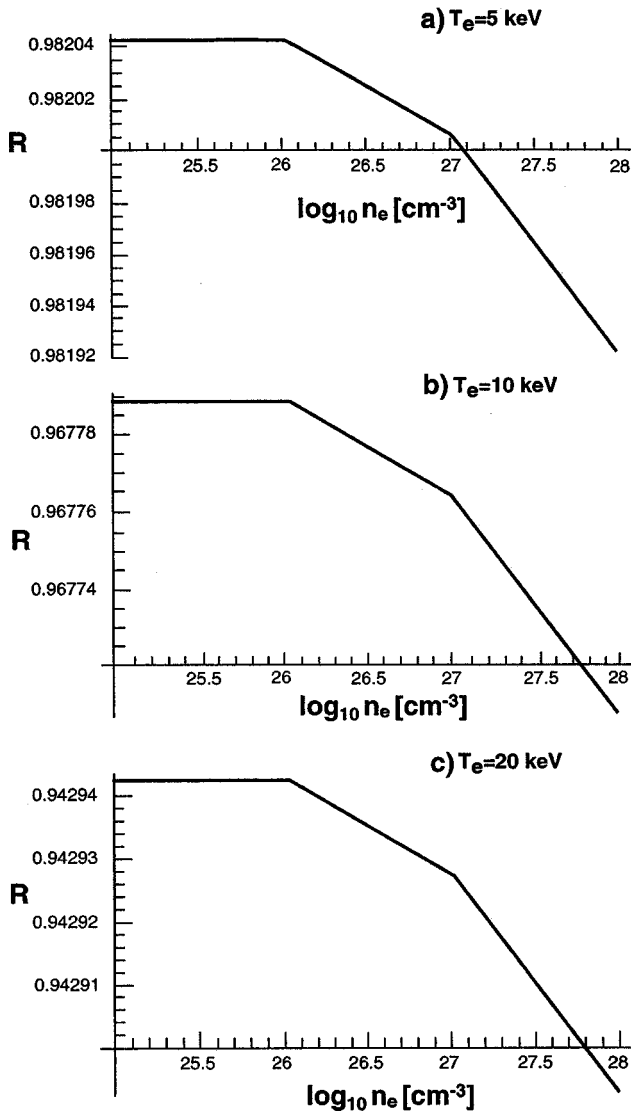


FIG. 3. Ratio  $R$  in terms of target electron density  $n_e$  for a dicorrelated projectile pair with  $r_{\parallel}=r_{\perp}=1\lambda_D$  and  $V=0.96c$  in a hydrogenic plasma. (a)  $T_e=5$  keV, (b)  $T_e=10$  keV, and (c)  $T_e=20$  keV.

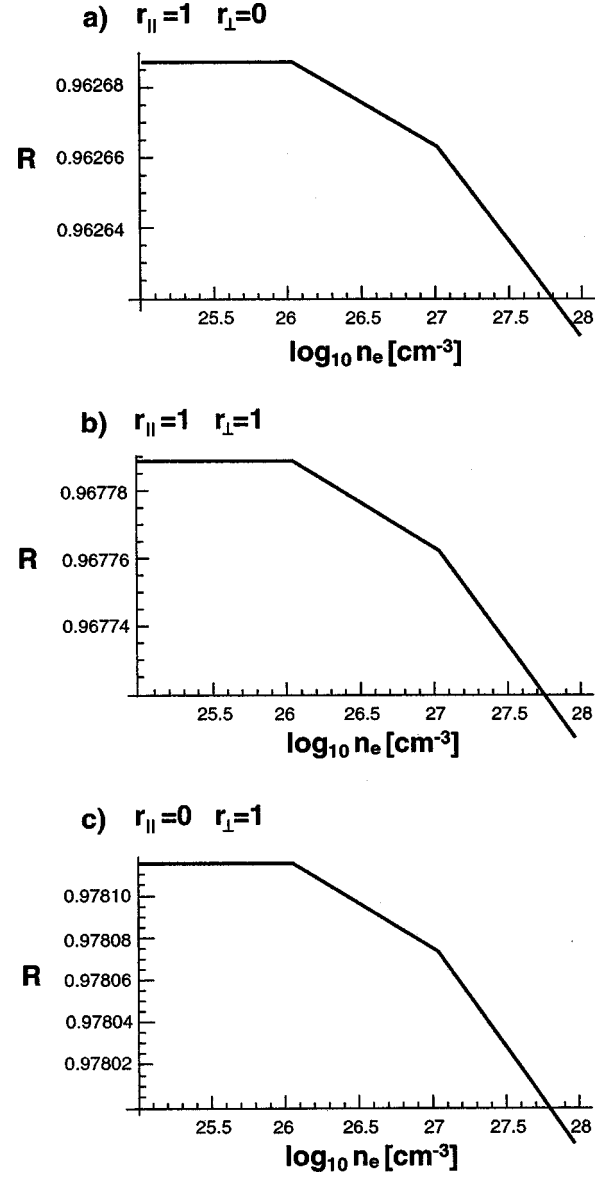


FIG. 4. Ratio  $R$  in terms of target electron density  $n_e$  for a dicorrelated electron pair in a hydrogenic plasma at  $T_e=10$  keV with  $V=0.96c$ . (a)  $r_{\parallel}=1\lambda_D$ ,  $r_{\perp}=0$ ; (b)  $r_{\parallel}=r_{\perp}$ ; (c)  $r_{\parallel}=0$ ,  $r_{\perp}=1\lambda_D$ .

$$\vec{P}(\omega) = \frac{1}{4\pi} [\varepsilon(\omega) - 1] \vec{E}(\omega) \quad (3)$$

and

$$\vec{M}(\omega) = \frac{1}{4\pi} [\mu(\omega) - 1] \vec{H}(\omega). \quad (4)$$

The work done by a cluster in passing through a slab of medium with thickness  $dz$  is then given by (see Fig. 1)

$$dE = N dz \int_{\Pi} dx dy \frac{1}{2\pi N} \int_0^{\infty} d\omega \omega [\text{Im} \varepsilon(\omega) |\vec{E}|^2 + \text{Im} \mu(\omega) |\vec{H}|^2]. \quad (5)$$

Therefore the energy loss per unit distance is ( $\text{Im} \mu=0$ )

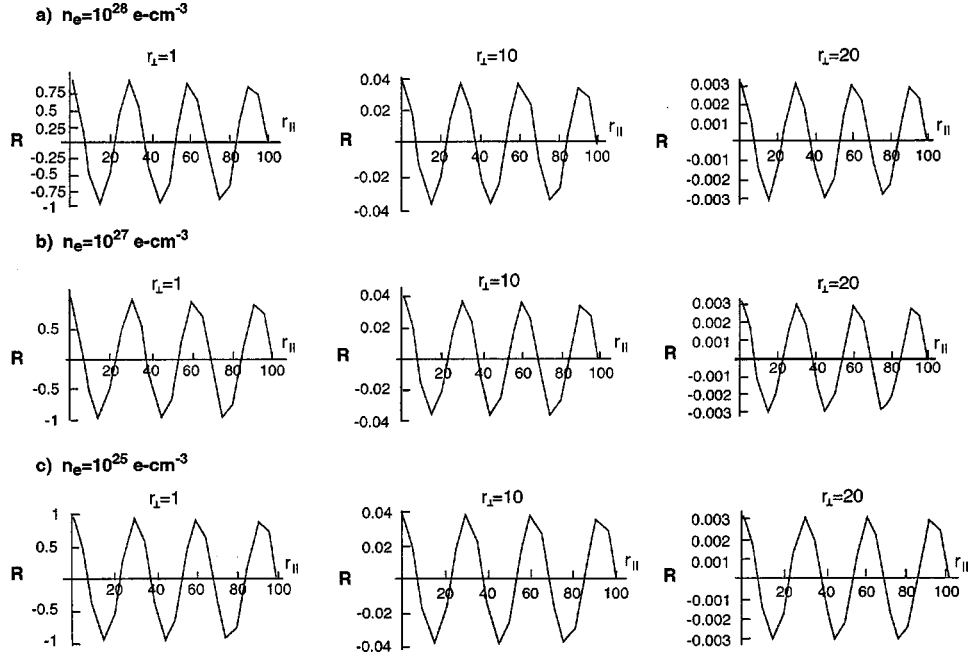


FIG. 5. Ratio  $R$  in a  $T_e = 20$  keV hydrogenic plasma. Transverse pair interdistance  $r_\perp$  is kept fixed, while  $r_\parallel$  is allowed to vary. (a)  $n_e = 10^{28} e \text{ cm}^{-3}$ , (b)  $n_e = 10^{27} e \text{ cm}^{-3}$ , and (c)  $n_e = 10^{25} e \text{ cm}^{-3}$ .

$$\frac{dE}{dz} = \frac{1}{2\pi} \int_{\Pi} dx dy \int_0^\infty d\omega \omega [\text{Im} \varepsilon |\vec{E}|^2 + \text{Im} \mu |\vec{H}|^2], \quad (6)$$

$$|\vec{E}|^2 = \left| \sum_{i=1}^n \vec{E}_i \right|^2 = \sum_{i=1}^n |\vec{E}_i|^2 + 2 \text{Re} \sum_{i < j} \vec{E}_i^* \cdot \vec{E}_j. \quad (8)$$

$$\frac{dE}{dz} = \frac{1}{2\pi} \int_a^\infty b db \int_0^{2\pi} d\phi \int_0^\infty \omega \text{Im} \varepsilon(\omega) |\vec{E}(\omega)|^2 d\omega \quad (7)$$

This form suggests defining the following stopping-power components  $dE_{ij}(\vec{R}_{ij})/dz$ , which are functions of the separation vectors  $\vec{R}_{ij}$ , from the  $i$ th to the  $j$ th particle in the cluster:

with

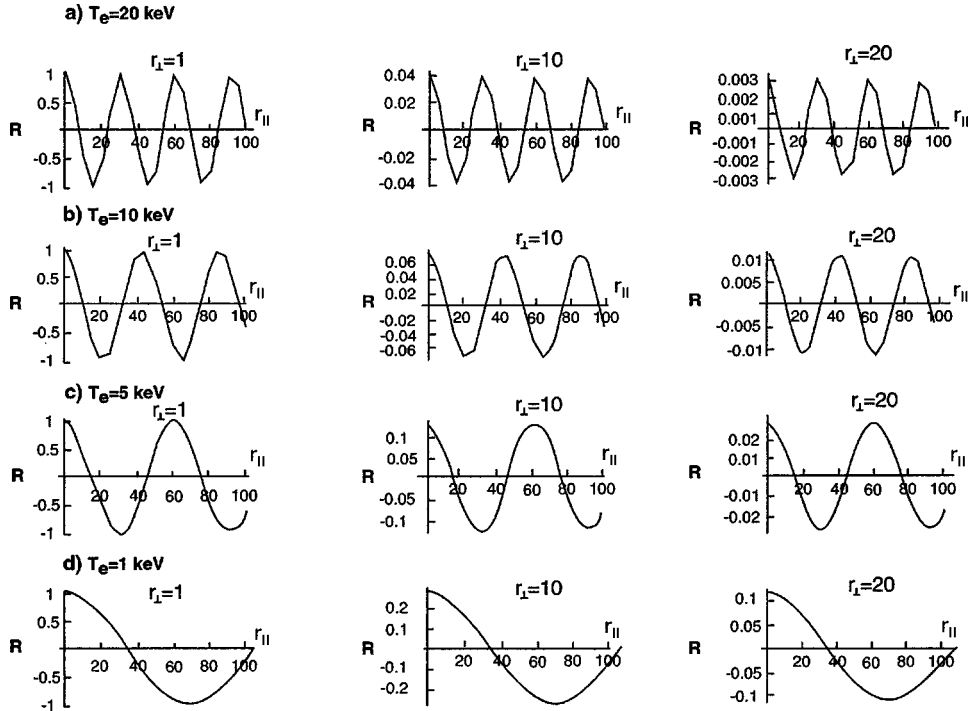


FIG. 6. Ratio  $R$  for a two-electron pair flowing in a  $n_e = 10^{26} e \text{ cm}^{-3}$  hydrogenic plasma with  $r_\perp$  fixed and varying  $r_\parallel$ . (a)  $T_e = 20$  keV, (b)  $T_e = 10$  keV, (c)  $T_e = 5$  keV, and (d)  $T_e = 1$  keV.  $V = 0.96c$ .

$$\frac{dE_{ii}}{dz} = \frac{1}{2\pi} \int_a^\infty b db \int_0^{2\pi} d\phi \int_0^\infty \omega \operatorname{Im} \varepsilon(\omega) |\vec{E}_i(\omega)|^2 d\omega, \quad (9)$$

and

$$\frac{dE_{ij}(\vec{R}_{ij})}{dz} = \frac{1}{2\pi} \int_a^\infty b db \int_0^{2\pi} d\phi \int_0^\infty \omega \operatorname{Im} \varepsilon(\omega) \operatorname{Re} \vec{E}_i^* \cdot \vec{E}_j(\omega) d\omega, \quad (10)$$

where  $a$  is the radius shown in Fig. 1. In the sequel we shall set  $a = \lambda_D$ .

The energy loss for an  $N$ -cluster can then be expressed as

$$\frac{dE}{dz} = \sum_{i=1}^N \frac{dE_{ii}}{dz} + \sum_{1 \leq i < j \leq N} \left( \frac{dE_{ij}}{dz} + \frac{dE_{ji}}{dz} \right) \quad (11)$$

in terms of the penetration distance  $z$  in target.

### III. DICORRELATED STOPPING

Scalar components of electric fields due to correlated electron projectiles 1 and 2 allow us to explicate [7] Eqs. (9)

and (10). For instance, the cross term in the integrand of Eq. (10) reads

$$\begin{aligned} \operatorname{Re} \vec{E}_i^* \cdot \vec{E}_j &= \frac{2}{\pi} \frac{Z_i Z_j e^2}{v_i v_j} \frac{1}{|\varepsilon|^2} \operatorname{Re} e^{-i\omega R_3/v_j} \\ &\times \left( \lambda_i^* \lambda_j \frac{(b-R_1)}{\rho} K_1(\lambda_i^* b) K_1(\lambda_j \rho) \right. \\ &\left. + \frac{v_i v_j}{\omega^2} (\lambda_i^*)^2 \lambda_j^2 K_0(\lambda_i^* b) K_0(\lambda_j \rho) \right), \quad (12) \end{aligned}$$

where  $\phi$  and  $b$  quadratures performed by Rule and Cha [7], finally allow for the dicorrelated stopping contribution

$$\frac{dE_c}{dz} = \frac{dE_{ij}(\vec{R}_{ij})}{dz} + \frac{dE_{ij}(\vec{R}_{ji})}{dz}. \quad (13)$$

Under the form

$$\begin{aligned} \frac{dE_c}{dz} &= \frac{2}{\pi} \frac{Z_i Z_j e^2}{v_i v_j} \int_0^\infty d\omega \omega \frac{\operatorname{Im} \varepsilon}{|\varepsilon|^2} \left( \operatorname{Re} e^{-i\omega R_3/v_j} \frac{\lambda_i^* \lambda_j}{\lambda_j^2 - \lambda_i^{*2}} \{ K_0(\lambda_j R_\perp) [\Lambda_{ji} b K_1(\lambda_i^* b) I_0(\lambda_j b) + \Lambda_{ij}^* b K_0(\lambda_i^* b) I_1(\lambda_j b)] \bar{a} \right. \\ &+ I_0(\lambda_j R_\perp) [\Lambda_{ij}^* \bar{a} K_1(\lambda_j \bar{a}) K_0(\lambda_i^* \bar{a}) - \Lambda_{ji} \bar{a} K_0(\lambda_j \bar{a}) K_1(\lambda_i^* \bar{a})] \} + \operatorname{Re} e^{-i\omega R_3/v_i} \frac{\lambda_j^* \lambda_i}{\lambda_i^2 - \lambda_j^{*2}} \{ K_0(\lambda_i R_\perp) \\ &\times [\Lambda_{ij} b K_1(\lambda_j^* b) I_0(\lambda_i b) + \Lambda_{ji}^* b K_0(\lambda_j^* b) I_1(\lambda_i b)] \bar{a} + I_0(\lambda_i R_\perp) [\Lambda_{ji}^* \bar{a} K_1(\lambda_i \bar{a}) K_0(\lambda_j^* \bar{a}) - \Lambda_{ij} \bar{a} K_0(\lambda_i \bar{a}) K_1(\lambda_j^* \bar{a})] \} \Big), \quad (14) \end{aligned}$$

with

$$\bar{a} \equiv \begin{cases} R_\perp, & R_\perp > a \\ a, & R_\perp < a \end{cases}$$

and

$$\Lambda_{ij} \equiv \lambda_i \left( \lambda_j^{*2} \frac{v_i v_j}{x^2 \omega_p^2} - 1 \right).$$

The single particle stopping pertaining to the first term in the right-hand side of Eq. (11) in the  $R \rightarrow 0$  limit, yields the Fermi expression [8]

$$\frac{dE_s}{dz} = Z^2 S, \quad (15)$$

where

$$S \equiv -\frac{2}{\pi} \frac{e^2}{v^2} \int_0^\infty d\omega \omega \operatorname{Im} \left[ K_0(\lambda_0 a) \left( \frac{1}{\varepsilon} - \beta^2 \right) \right] \quad (16)$$

and

$$\lambda \equiv \frac{|\omega|}{v} (1 - \beta^2 \varepsilon)^{1/2}.$$

### IV. TARGET DIELECTRIC FUNCTION

In view of the very high velocity regime of present concern, it appears appropriate to qualify the supercompressed electron target with a dispersion-free dielectric function, which reads as

$$\varepsilon(\omega) = 1 - \frac{\omega_p^2}{\omega(\omega + i\nu_{\text{coll}})} \quad (17)$$

in a Drude form suitable for high-velocity REBs with a collision frequency

$$\nu_{\text{coll}} = \frac{3.8 \times 10^{-6} [n_e (\text{cm}^{-3})]}{[T_e (\text{eV})]^{3/2}} \ln \Lambda, \quad (18)$$

given in terms of plasma parameters. For the case of a deuterium+tritium (DT) thermonuclear fuel compressed at  $300 \text{ g/cm}^3$ , one has

$$\ln \Lambda = \ln[9n_e \lambda_D] = 6.305$$

with  $T=5 \text{ keV}$  and  $n_e = 10^{26} \text{ e cm}^{-3}$ .

It is also useful to recognize that the  $k$ -independent expression (17) fulfills exactly the  $\omega$ -sum rule

$$\int_0^\infty d\omega \omega \operatorname{Im} \frac{1}{\varepsilon(\omega)} = -\frac{\pi}{2} \omega_p^2. \quad (19)$$

## V. CORRELATED STOPPING

In order to assess quantitatively the significance of the presently considered long ranged correlations, we now pay attention to the ratio

$$R = \frac{dE_c/dz}{2dE_s/dz} \quad (20)$$

of the right-hand side of Eqs. (14) and (16), respectively, with the target dielectric function (17).

We now intend to document numerically the basic features and trends of the dicorrelated stopping ratio  $R$  [Eq. (20)]. In connection with the interaction physics of the fast-

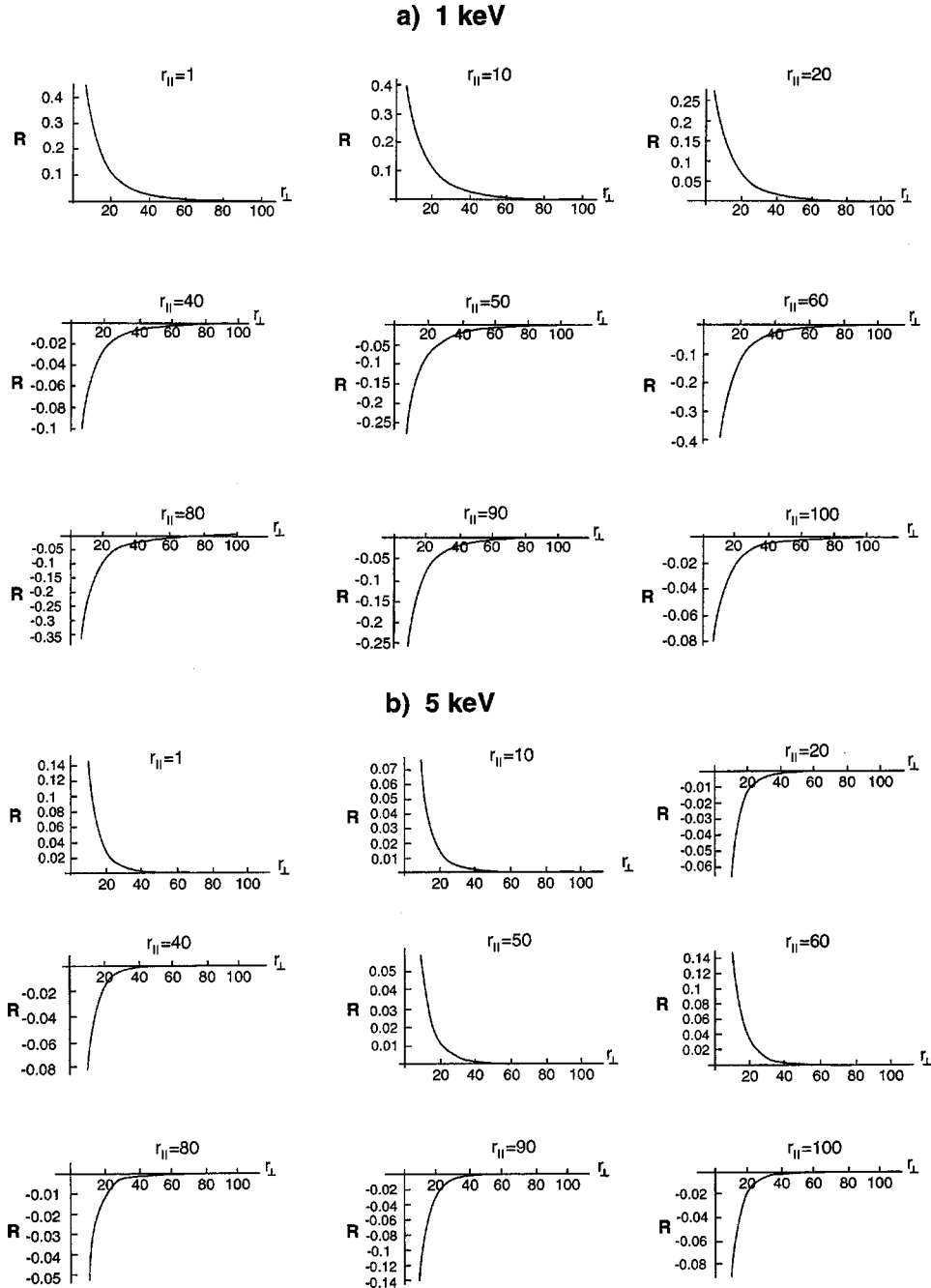
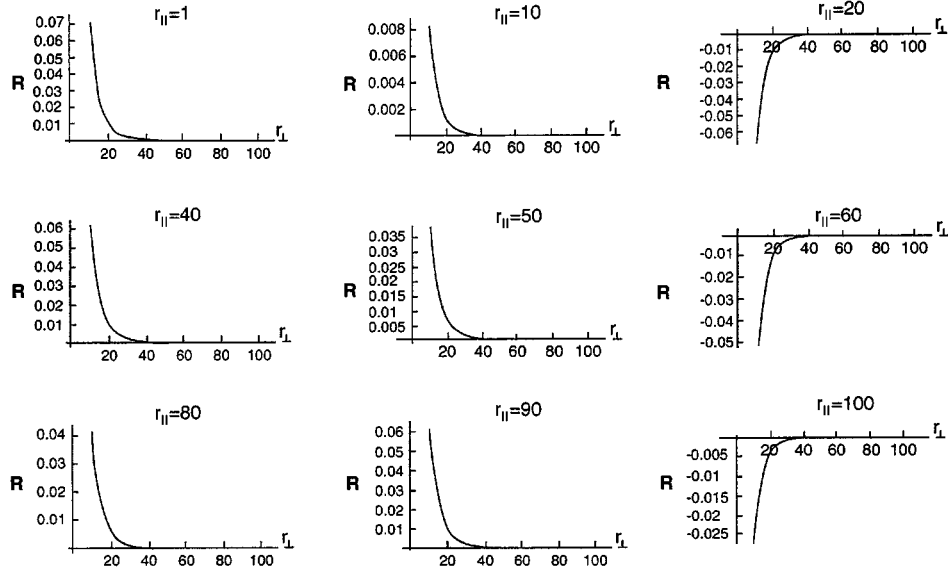


FIG. 7. Same caption as in Fig. 5 with  $r_{\parallel}$  and  $r_{\perp}$  permuted. (a)  $T_e = 1 \text{ keV}$ , (b)  $T_e = 5 \text{ keV}$ , (c)  $T_e = 10 \text{ keV}$ , and (d)  $T_e = 20 \text{ keV}$ .  $V = 0.96c$ .

## c) 10 keV



## d) 20 keV

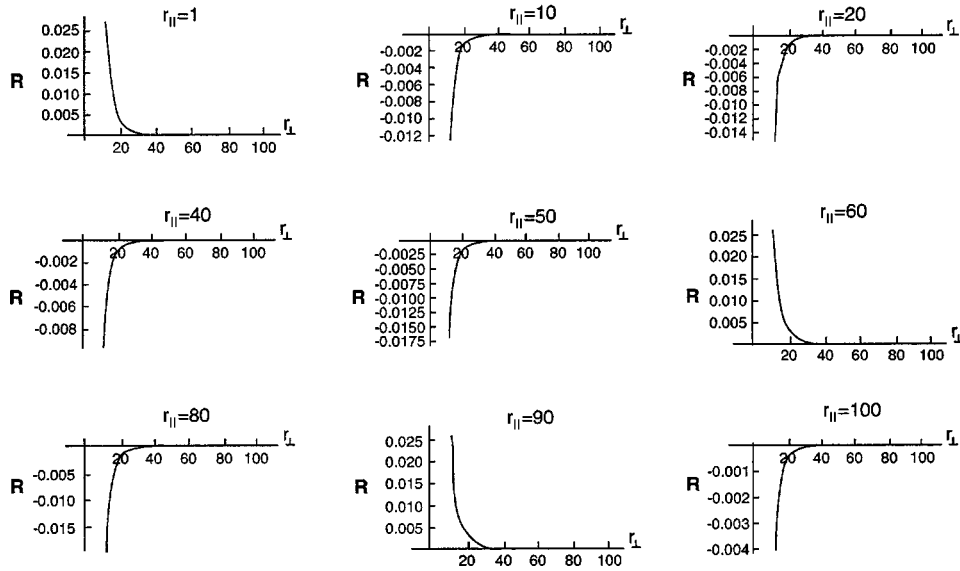


FIG. 7. (Continued).

ignitor scenario we stress correlated stopping of relativistic electron pairs with overall drift velocity  $V=0.96c$  (kinetic energy/electron=3.084 MeV) slowing down in a very dense hydrogenic plasma with  $10^{25} \leq n_e \leq 10^{28} e \text{ cm}^{-3}$  density and temperature  $T_e \geq 1 \text{ keV}$ . Pair interdistances are, respectively, taken parallel ( $r_{\parallel}$ ) and transverse ( $r_{\perp}$ ) to  $\vec{v}$ . They are measured in number of target electron Debye length  $\lambda_D$ . In the nomenclature used in Eq. (14) one has to read now  $r_{\parallel} \equiv R_{\parallel}$  and  $r_{\perp} \equiv R_{\perp}$ .

## A. Overall behavior

Figures 2 and 3, respectively, highlight  $T_e$  and  $n_e$  trends for a typical projectile pair oriented at  $\pi/4$  with respect to  $\vec{v}$ . Both captions demonstrate that the correlated stopping ratio

$R$  decreases with increasing target temperature at fixed  $n_e$ . Otherwise stated,  $R$  increases with target plasma parameter  $\Lambda_e = e^2/k_B T_e \lambda_D$ . Moreover, Figs. 2 and 3 show unambiguously that  $R$  has practically no  $n_e$  variations in the given range of interest. It remains constant to within four digits for a given pair orientation. On the other hand, Figs. 4 advocate the usual orientation hierarchy with maximum correlated stopping for transverse pair [see Fig. 3(c)], already observed at nonrelativistic velocities  $V$ .

B.  $n_e$  behavior

The insensitivity of  $R$  to  $n_e$  variations is made even more conspicuous in Figs. 5 with  $r_{\perp}$  fixed and increasing  $r_{\parallel}$  for several  $n_e$  values in a  $T_e = 20 \text{ keV}$  hydrogenic plasma and

with the same projectile velocity, as above. What appears even more striking is the repetition of an identical oscillatory pattern when  $r_{\perp}$  is changed, whatever  $n_e$  may be. The given  $R_{\parallel}$  pattern is again rigorously reproduced at  $n_e = 10^{26} \text{ e cm}^{-3}$  and  $T_e = 20 \text{ keV}$  [Fig. 6(a)].

### C. $T_e$ variations

Keeping  $n_e = 10^{26} \text{ e cm}^{-3}$  (Figs. 6) and varying  $T_e$  between 1 and 20 keV results in a very different picture. The oscillation period decreases significantly with  $T_e$  while  $|R|$  increases by orders of magnitude between 20 and 1 keV, when  $r_{\perp} > \lambda_D$ . Permuting now  $r_{\parallel}$  with  $r_{\perp}$ , and keeping  $r_{\parallel}$  fixed, while  $r_{\perp}$  runs up to  $100\lambda_D$  produces monotonous decaying (or increasing patterns) according to the sign of  $R$  (see Figs. 7).  $|R|$  remains nonnegligible on a largest  $r_{\perp}$  range at lowest  $T_e$  value (largest coupling  $\Lambda_e$ ). Going back to expres-

sion (14), it appears immediately that the  $K_0(x)$  factors are monitoring the presently noticed monotonous behavior, while  $R$  changes sign through harmonic terms. Here, also,  $|R|$  decays by orders of magnitude from 1 up to 20 keV.

### VI. SUMMARY

We proceeded to a thorough investigation of dicorrelated stopping for pairs of relativistic electrons interacting with an ultradense, albeit weakly coupled, hydrogenic plasma of ICF interest. Modeled with a Drudelike dielectric function, correlation effects [14] have been shown to be non-negligible through the stopping ratio  $R$  [Eq. (20)] over several tens of target electron screening lengths. They are often of the order of isolated, uncorrelated stopping contributions (16).  $R$  exhibits more sensitivity to temperature than to density variations, as far as target parameters are concerned.

- 
- [1] M. Tabak, J. Hammer, M. E. Glinsky, V. L. Kruer, S. C. Wilks, J. Woodworth, E. M. Campbell, M. D. Perry, and R. J. Mason, *Phys. Plasmas* **1**, 626 (1994).
  - [2] C. Deutsch, H. Furukawa, K. Mina, M. Murakami, and K. Nishihara, *Phys. Rev. Lett.* **77**, 2489 (1996); *Laser Part. Beams* **15**, 577 (1997).
  - [3] A. Bret and C. Deutsch, *Phys. Rev. E* **47**, 1276 (1993).
  - [4] C. Deutsch and P. Fromy, *Phys. Rev. E* **51**, 632 (1995).
  - [5] M. Kitagawa and Y. H. Ohtsuki, *Phys. Rev. B* **16**, 5321 (1977).
  - [6] M. Lontano and F. Raimondi, *Phys. Rev. E* **51**, R2755 (1995).
  - [7] D. W. Rule and M. H. Cha, *Phys. Rev. A* **24**, 55 (1981).
  - [8] E. Fermi, *Phys. Rev.* **57**, 485 (1940).
  - [9] J. D. Jackson, *Classical Electrodynamics*, 2nd ed. (Wiley, New York, 1975), Chap. 13.